Role of Heme in Structural Organization of Cytochrome *c* Probed by Semisynthesis[†]

Xinshan Kang and Jannette Carey*

Department of Chemistry, Princeton University, Princeton, New Jersey 08544-1009

Received August 16, 1999; Revised Manuscript Received October 11, 1999

ABSTRACT: The heme prosthetic group of cytochrome *c* is covalently attached to the protein through thioether bonds to two cysteine side chains. The role of covalent heme attachment to cytochrome *c* is not understood, and most heme proteins bind the prosthetic group by iron ion ligation and tertiary interactions only. A two-armed attachment seems redundant if the role of covalent connection is to limit heme group orientation or to decouple heme affinity from redox potential. These considerations suggested that one role for covalent attachment of the rigid planar heme might be in organizing the cytochrome *c* protein structure. Indeed, porphyrin cytochrome *c* (in which the heme iron ion has been removed) is substantially more ordered than apocytochrome *c*, having characteristics consistent with a molten globule state. To assess the importance of planar rigidity in ordering this protein, semisynthesis was used to substitute porphyrin by two hydrophobic surrogates, one based on biphenyl and the other on phenanthrene, which have different degrees of planarity and rigidity. The expected two-armed covalent attachment of each surrogate was confirmed in the protein products by a variety of methods including mass spectrometry and NMR. Despite being only about half the size of the porphyrin macrocycle, and lacking any possibility for ligation or polar group interactions with the surrounding protein, the two surrogates confer helix contents that are comparable to that of the molten globule formed by porphyrin cytochrome *c* under similar solution conditions. The pH titrations of the derivatives monitored by circular dichroism exhibit reversible, bell-shaped folding and unfolding transitions, implying that charge group interactions in the protein are involved in stabilizing the helical structures formed. The thermal transitions of the two derivatives at neutral pH are cooperative, with similar midpoints. The similarity of helical content and structural stability in the two derivatives indicates that the increase in conformational freedom by the biphenyl surrogate does not substantially reduce protein structural stability. The similarity of the two derivatives to porphyrin cytochrome *c* suggests that the common feature among the three covalently attached groups—their hydrophobicity—is by far the dominant factor in organizing stable structures in the protein.

Horse heart cytochrome *c* (cyt *c*) is a small heme protein with 104 amino acid residues and is an important electron-transfer protein in the respiratory chain. The three-dimensional native structure of this protein has been well-characterized by both X-ray crystallography (*1, 2*) and MNR spectroscopy (*3, 4*), and consists of a compact core around the heme moiety (Figure 1). Two main helices, the N- and C-terminal helices, intersect near their centers on one side of the heme plane. The heme prosthetic group is covalently attached by heme lyase during mitochondrial import (*5*) through thioether links to cysteines 14 and 17 just beyond the end of the N-terminal helix. An irregularly structured chain segment comprising residues 19−38, and the proximal heme ligand His18, completes the tertiary fold on this side of the heme plane. On the other side of the heme, the fold is formed by extensive irregularly structured segments, two short helices, and the distal heme ligand Met80.

The heme group in cyt *c* is not only the redox center of the protein, but is also critical for maintaining the native structure: its removal causes disruption of the native fold and loss of most of the secondary structure under physiological conditions (neutral pH values and low salt concentration; *6*−*10*). In other hemoproteins, such as cytochromes b_5 (*11*−*14*) and b_{562} (*12*) and myoglobin (*13*, *14*), the apoproteins retain nativelike secondary and tertiary structural features except near the heme-binding site. In all these

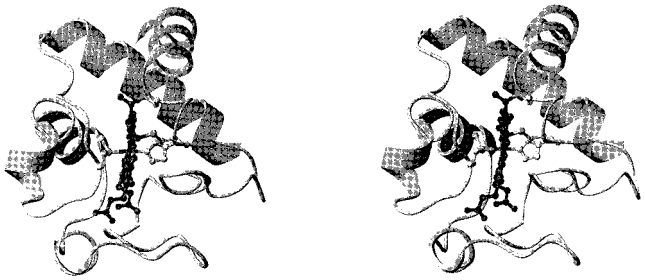

FIGURE 1: Stereopair showing the three-dimensional structure of horse heart cytochrome *c*. The polypeptide backbone of residues forming helices is shown as a ribbon, and the remaining residues are represented by a string. The heme and its connecting residues Cys14, Cys17, His18, and Met80 are shown in ball-and-stick models. The N-terminus is located at the top back of the molecule and the C-terminus at the middle right. The model was constructed from file 1hrc.pdb from the Brookhaven Protein Data Bank using the program MOLMOL (*39*).

[†] Supported by Grant NIH GM43558 to J.C.

* Corresponding author. Telephone: (609) 258-1631. FAX: (609) 258-6746. E-mail: carey@chemvax.princeton.edu.

10.1021/bi9919089 CCC: $18.00
Published on Web 11/10/1999

proteins, including cyt *c*, the heme group forms extensive interactions with the surrounding protein. In addition to its axial ligands, interactions between the two heme propionate groups and polar residue side chains nearby, and hydrophobic interactions between the porphyrin ring and buried nonpolar side chains are observed in the native structures. These interactions reflect common contributions of the heme group to structural maintenance in all its host proteins. Consistent with these features, exogenously added heme can induce a compact and helical, but highly dynamic, state in apocytochrome *c* when bound only by iron ion ligation and tertiary interactions, but not by thioether linkages (*15*, *16*). Alternatively, disruption of the heme axial ligands alone is sufficient to render porphyrin cytochrome *c* (ppcc) a molten globule except under extreme solution conditions (*10*).

The requirement for covalent attachment of the heme group to the cysteine side chains in functional cyt *c* is not understood. Covalent attachment could serve to restrain the prosthetic group with higher specificity than could be achieved solely by oriented ligations as in other hemoproteins, which in some cases display heme orientational disorder (*17*, *18*). However, this is not likely the only reason for the covalent attachment of the heme group in cyt *c*, which is attached not just once, but twice in the vast majority of cytochromes *c*. Though little is known about heme lyase, a requirement for bidentate heme attachment arising from its catalytic mechanism seems to be ruled out by two key observations: a small number of cytochromes *c* have only a single thioether linkage (*19*), and a human cytochrome *c* mutant with one of the cysteine residues replaced by alanine retains the heme group and is partly functional in yeast (*20*, *21*).

Taken together with the rigid planarity of the heme moiety, its double attachment suggests the possibility that it plays a structural role in the proteins to which it is covalently attached. This role could involve organization of the protein's fold and/or transmission of redox-linked conformational changes. It has been observed that asymmetric, nonplanar distortion of the heme ("ruffling") is conserved in cytochromes *c* and is proposed to be induced by heme covalent attachment and enforced by the protein's tertiary structure (*22*); heme ruffling during the redox cycle may be communicated through the protein via these connections. Heme attachment also may significantly restrict the backbone conformation of the short segment Cys14-Ala15-Gln16-Cys17 (horse heart numbering and most frequently observed sequence among species). Such restriction could lower the entropy difference between the native and unfolded states by an estimated maximum of 2 kcal/mol (calculated as described in ref *23*), and may also enforce specific functional group interactions within the protein and/or between the protein and heme.

Close examination of the sequences of three cytochromes *c* having only one thioether link [one from *Euglena gracilis* and two from Crithidians (*19*)] reveals that they present only conservative substitutions in buried residues that contact the heme (residues 35, 64, 67, 85, 95, and 98 in horse heart numbering), indicating that no simple and direct sequence compensation apparently correlates with loss of one thioether link. However, more drastic sequence changes are found in these three proteins at several other positions (12, 20, 21, 27, 75, 81, and 101), some of which are fully or partly buried

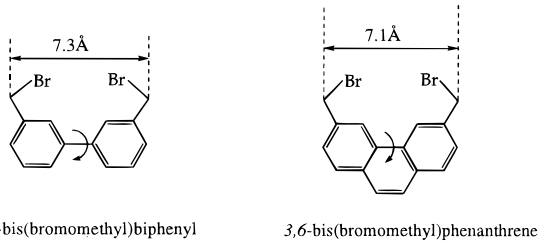

FIGURE 2: Structures of the two surrogate groups used in the present work. The arrows indicate the bonds discussed in the text.

(20, 75, 81) and/or highly conserved in the majority of other species (27, 75); some of the observed substitutions are unique, or nearly unique, to the three species with single thioether links. These observations suggest the possibility that some of these residues may comprise a covarion (*24*) in the context of the Cys14 to Ala substitution. Detailed study of the Euglena ferricytochrome *c*, which bears the substitution Cys14 to Ala and only one thioether link, by Brems and Stellwagen (*25*) found no significant perturbations of its refolding mechanism relative to the horse heart protein. Rate constants for measurable folding steps of the Euglena protein were consistent with its equilibrium stability, which is lower than that of the horse heart protein by an amount that could be explained quantitatively by its amino acid sequence differences. Thus, results available to date do not elucidate the role of heme covalent attachment.

The present study examines the role of covalent attachment in structural organization of horse heart cyt *c* by replacing the porphyrin group with two heme surrogates differing in planarity and flexibility. The two surrogates, *m,m′*-bis(bromomethyl)biphenyl and 3,6-bis(bromomethyl)phenanthrene (Figure 2), are capable of reacting chemically to form thioether linkages with the cysteine side chains of apocytochrome *c*, through loss of their bromine atoms upon reaction with the cysteine thiolates. The calculated distance between the two connecting bromomethyl groups for each surrogate (7.1 or 7.3 Å) is similar to the distance between the two connecting groups on protoporphyrin IX (7.2 Å). Therefore, the double connections from the surrogates to the two cysteines model the similar attachments of the porphyrin group in holocytochrome *c*. The two compounds apply a large difference in the degree of free rotation about the central bond of the surrogate. The preferred dihedral angle between the two benzene rings of biphenyl is 40.4°, and rotation around the bond between the two benzene rings has a relatively low free energy cost [less than 2.2 kcal/mol to rotate to 0°; (*26*)]. Phenanthrene adopts a planar structure, and rotation of the dihedral angle by 40° costs at least 6 kcal/mol. Thus, phenanthrene may apply greater restriction to the polypeptide conformation in the short segment between Cys14 and Cys17, which may favor formation of folded structure by entropic destabilization of the unfolded state and/or by specific functional group interactions. Being approximately half the size of the porphyrin ring, each surrogate also maintains at least part of the hydrophobic quality of the porphyrin, but the surrogates are unable to form either axial coordinations or polar interactions with the surrounding protein as heme does. Whether the surrogates are able to organize the protein structure as porphyrin does may thus provide some insight into the structural roles of covalent attachment: similarities and differences among ppcc, bpcc,

and phcc may shed some light on the structural significance of the planarity and rigidity of the covalently attached group.

MATERIALS AND METHODS

Synthesis of 3,6-Bis(bromomethyl)phenanthrene. Five hundred milligrams (2.42 mmol) of 3,6-dimethylphenanthrene (Aldrich) was dissolved in 30 mL of carbon tetrachloride, and 890 mg (5.06 mmol) of *N*-bromosuccinimide (NBS) was added. The solution was stirred under irradiation from a 250 W tungsten lamp and heated to reflux for 10 h. The yellowish solution was cooled and washed with water 3 times. The turbid carbon tetrachloride layer was gently shaken with solid sodium sulfate until clear. The salt was filtered off and the filtrate taken to dryness on a rotary evaporator. The yellow solid was dissolved in a small amount of hot benzene and slowly cooled to room temperature. The supernatant was removed, and the solid was recrystallized from chloroform. The final needlelike crystals were dried under vacuum overnight.

Synthesis of m,m′-Bis(bromomethyl)biphenyl. *m,m′*-Dimethylbiphenyl (Aldrich) was reacted similarly as for 3,6-di(bromomethyl)phenanthrene (*26*). Ten grams (0.055 mol) of *m,m′*-bismethylbiphenyl, 20.4 g (0.116 mol) of NBS, and 0.4 g (0.0016 mol) of benzoyl peroxide were dissolved in 40 mL of carbon tetrachloride and refluxed at 80 °C for 5 h. The reaction mixture was filtered while still hot, the cooled filtrate was washed with water 3 times, and the carbon tetrachloride layer was dried with sodium sulfate and allowed to stand in a desiccator overnight. The resulting crystals were recrystallized from benzene and dried under vacuum.

Synthesis of Phenanthrene and Biphenyl Cytochrome c Derivatives. Apocytochrome *c* (see Figure 3C) was prepared as described (*7*, *27*) from horse heart cytochrome *c* (Sigma Chemical, type VI, C-7752). One milligram (0.08 mmol) of apocytochrome *c* was dissolved in 1 mL of 5 mM Tris·HCl buffer, pH 5.0. Then 13 μL (0.08 mmol) of 1 mg/mL dithiothreitol was added and stirred at room temperature under nitrogen for 1.5 h; 17 μL of 1.5 M Tris base was added to adjust the pH value to 8.8, and immediately 65 μL of 1 mg/mL 3,6-bis(bromomethyl)phenanthrene (0.18 μmol) or 61 μL of 1 mg/mL *m,m′*-bis(bromomethyl)biphenyl (0.18 μmol) was added from stock solution in ethanol. The reaction mixture was stirred at room temperature under nitrogen for 4.5 h. The reaction was stopped by adding 10−15 μL of glacial acetic acid to adjust the pH of the turbid solution to approximately 5, and the solution turned nearly transparent. The reaction mixture was dialyzed (MWCO, 3800 Da) exhaustively against 20 mM ammonium acetate, pH 9, at 4 °C and clarified by centrifugation.

Purification of Phenanthrene and Biphenyl Cytochrome c Derivatives. A carboxymethyl (CM) Sephadex C-25 column (20 × 1 cm, volume 15 mL) was equilibrated in 0.3 M NH_4OAc, pH 9.0 at 4 °C, the dialyzed reaction solution was loaded, and the column was eluted using a hyperbolic concentration gradient of ammonium acetate, pH 9.0 (30 mL of 0.3 M + 45 mL of 1.5 M). The combined fractions of purified derivative proteins (see Results) were lyophilized and stored at −20 °C.

Spectroscopy. Absorption spectra were obtained on a Hewlett-Packard 8452a diode array UV−visible spectrophotometer at room temperature. The two heme surrogates *m,m′*-bis(bromomethyl)biphenyl and 3,6-bis(bromomethyl)phenanthrene were examined on a Kratos MS 50 high-resolution spectrometer in the electron impact mode. The two cyt *c* derivatives were evaluated on a Hewlett-Packard 5989B (Electrospray) MS Engine.

Determination of Free Sulfhydryl Groups. The DTNB assays followed previously reported procedures (*28*). Fifty milliliters of protein (60 mM in deionized water) was mixed with 16 μL of 100 mM Tris·HCl, pH 9.0, and 16 μL of 3 mM DTT, and incubated at room temperature for 25 min. Then 382 μL of $NaAsO_2$ (2.6 mM in 200 mM Tris·HCl, pH 8.1) was added and incubated for 5 min, and 16 μL of DTNB stock (3 mM in 50 mM sodium acetate, pH 5.0) was added. The absorbance at 412 nm was immediately recorded every 5 s for 5 min. The linear portion of the curve was extrapolated back to the time of adding DTNB, corrected by subtraction of the value obtained for a blank sample, and converted to the thiol concentration using an extinction coefficient of 1.36×10^4 M^{-1} cm^{-1}.

Protein Concentration and Extinction Coefficient Determination. Protein concentrations determined by ninhydrin assay (*29*) using a calibrated stock of leucine as a standard (*30*) were used to determine the extinction coefficients.

Circular Dichroism. CD spectra were recorded on an Aviv model 62DS spectropolarimeter at 20 °C in a 2 mm pathlength cell with 1.0 nm bandwidth, stepsize of 1 nm, and averaging time of 2 s for each data point. All samples were scanned 3 times, and the average spectra were used. For pH titrations, protein samples were initially dissolved at 6−35 μM in 10 mM sodium phosphate, pH 2.6, and the pH value was adjusted by addition of 0.1 N NaOH or 0.7% HCl. pH values were measured with an error of ±0.1 using an Orion Research analogue pH meter model 301 with an Aldrich pH electrode Z11343-3. Helix content was calculated by the multilinear regression analysis method as described by Greenfield (*31*) using all the ellipticity data between 190 and 240 nm. The use of both three- and four-component standard curve sets was evaluated for deconvoluting the experimental data, including contributions from helix, turn, random, and optionally strand. The calculated helix content differed by approximately 5% with and without inclusion of strand contributions, and this difference is of the same order of magnitude as the known error in estimating helix content from the MLR method. Thus, calculated helix contents are reported here with an error of ±5%.

NMR Spectroscopy. NMR spectra were acquired at 25 °C on a 600 MHz Varian Unity/INOVA spectrometer equipped with three-axis gradients. Protein samples (200−300 μM in 10 or 20 mM sodium phosphate, pH 6.0) were prepared in D_2O or deionized H_2O. Two-dimensional (2D), gradient-selected, homonuclear multiple quantum coherence (HoMQC) spectroscopy with excitation delays between 10 and 200 ms (*32*) and nuclear Overhauser effect spectroscopy (NOESY) with mixing times of between 60 and 200 ms (*33*) were recorded. Water signals were suppressed by using the WATERGATE pulse scheme (*34*). Offline data processing, visualization, and analysis of 2D spectra used NMRPipe (*35*) and NMRView (*36*).

RESULTS

Synthesis of Biphenyl and Phenanthrene Bromomethyl Heme Surrogates. Synthesis of biphenyl and phenanthrene

bromomethyl derivatives started from commercially available *m,m′*-dimethylbiphenyl and 3,6-dimethylphenanthrene. The single bromination of each of the two methyl groups of the biphenyl or phenanthrene compounds was carried out by reacting with *N*-bromosuccinimide in a reaction initiated by light. The recrystallized products, *m,m′*-bis(bromomethyl)-biphenyl and 3,6-bis(bromomethyl)phenanthrene, obtained in approximately 60 and 50% yields, respectively, were confirmed by 1D ^{1}H NMR spectroscopy and mass spectrometry (*30*).

Synthesis and Purification of Cytochrome c Derivatives. Apocytochrome *c* was reacted with each heme surrogate in 50 mM Tris buffer at pH 9. The reaction mixtures turned turbid as the reaction proceeded, indicating that the products dissolve less well than the reactants. Unreacted apocytochrome *c* was removed on a weak cation-exchange column (CM Sephadex C-25) at pH 9.0. This pH favors the deprotonation of free cysteine residues, and thus unreacted apocytochrome *c* is expected to elute earlier than the substituted cytochromes *c* because of its greater negative charge. The column profiles (Figure 3) consistently showed two well-separated peaks. The first peak in each case had a UV spectrum with a maximum at 280 nm, while fractions in the second peak had changes in line shapes and shifted maxima consistent with the presence of the surrogates. Pooled fractions from each second peak were repurified on the ion exchange column under identical conditions.

DTNB assays showed that the fractions from the earlier eluting peaks had an average of 1.7 ± 0.2 free sulfhydryl groups per molecule, whereas fractions from the later eluting peak for each derivative showed negligible free sulfhydryl content, indicating that both cysteine residues are occupied in each derivative molecule. To differentiate between the expected derivatives incorporating just one surrogate group by double attachment to one protein molecule and the possible byproducts incorporating two surrogate groups at the two cysteines, ESI mass spectra of the two derivatives were determined. The results showed *m/z* values of 11 922 for biphenyl−cytochrome *c* (bpcc) and 11 946 for phenanthrene−cytochrome *c* (phcc). These values fit well within experimental error to the values expected (11 918 ± 12 and 11 942 ± 12, respectively) for incorporation of each surrogate with two attachments to one protein, thus excluding byproducts with two surrogates in one protein chain. Therefore, the substituted groups were correctly introduced into apocytochrome *c* with the two-armed attachment to the cysteines as expected. The overall yield of the purified, doubly attached products with respect to apocytchrome *c* averaged approximately 15−25% for either derivative.

The concentrations of the two cytochrome *c* derivatives were determined by ninhydrin assays with an error of ±20%. The extinction coefficients were then calculated from their UV spectra in 10 mM sodium phosphate buffer, pH 7.0. Absorbance spectra are shown in Figure 3C. Biphenyl−cytochrome *c* has extinction coefficients of (1.4 ± 0.3) × 10^4 M^{-1} cm^{-1} at 280 nm, (1.6 ± 0.3) × 10^4 M^{-1} cm^{-1} at 276 nm, and (1.6 ± 0.3) × 10^4 M^{-1} cm^{-1} at 260 nm with no distinctive peaks. Phenanthrene−cytochrome *c* has peaks at 262 nm with extinction coefficient (6.0 ± 1.2) × 10^4 M^{-1} cm^{-1}, at 306 nm with extinction coefficient (2.3 ± 0.5) × 10^4 M^{-1} cm^{-1}, and at 276 nm with extinction coefficient (3.5 ± 0.7) × 10^4 M^{-1} cm^{-1}.

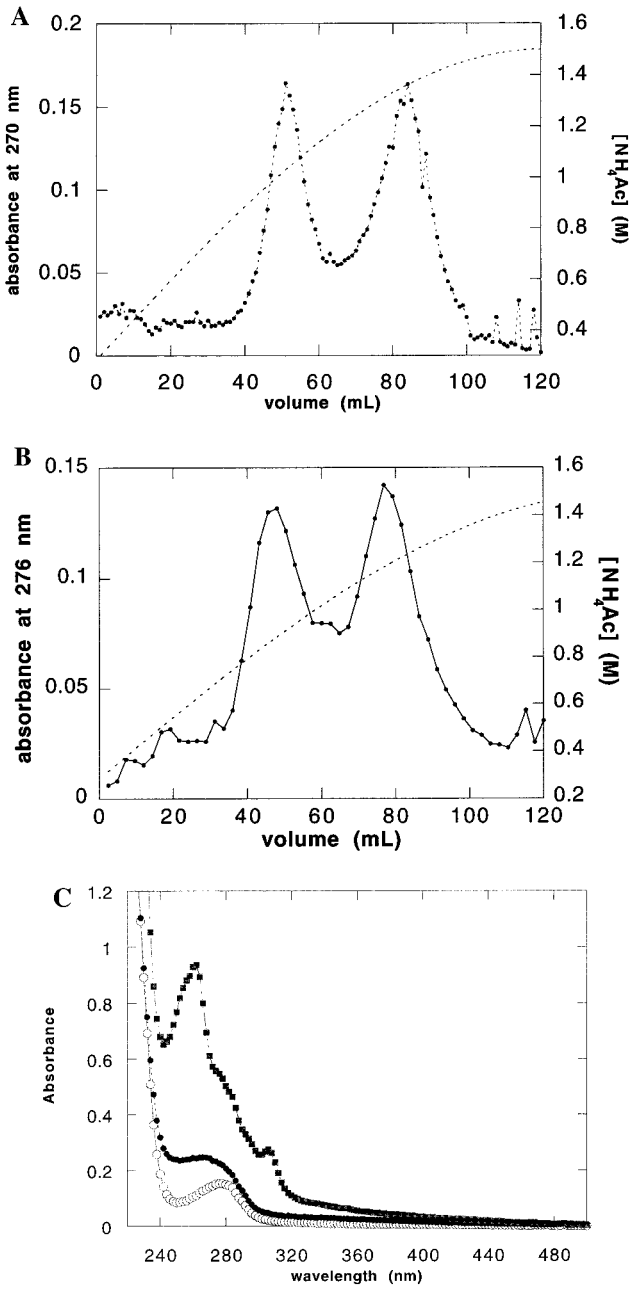

FIGURE 3: Purification of semisynthetic cytochrome *c* derivatives. Panels A and B show the elution profiles of bpcc and phcc reaction mixtures, respectively, from a carboxymethyl Sephadex column. The column was developed with a hyperbolic gradient of ammonium acetate, pH 9 (- - -), from 0.3 to 1.5 M. Protein content of the fractions (●) was determined by measuring absorbance at 270 nm in (A) or at 276 nm in (B). Panel C shows absorbance spectra of the starting material apocytochrome *c* (○), and of the twice-purified bpcc (●) and phcc (■) at 16 μM in 10 mM sodium phosphate, pH 6.0.

One-dimensional ^{1}H NMR spectra of the two substituted cytochrome *c* derivatives at 600 MHz in D_2O showed extra peaks in the aromatic chemical shift region compared to that for apocytochrome *c*. One- and two-dimensional spectra were acquired at pH 3 to shift the peaks of the histidine C_2 protons downfield from about 7.7 ppm to 8.6 ppm, to avoid overlap with the proton signals from the attached surrogates. Assignments of aromatic protons of the surrogate groups were made by comparing 1D spectra for bpcc and phcc with those for the free surrogates, and by analysis of the 2D-HoMQC and NOESY spectra of the derivatives.

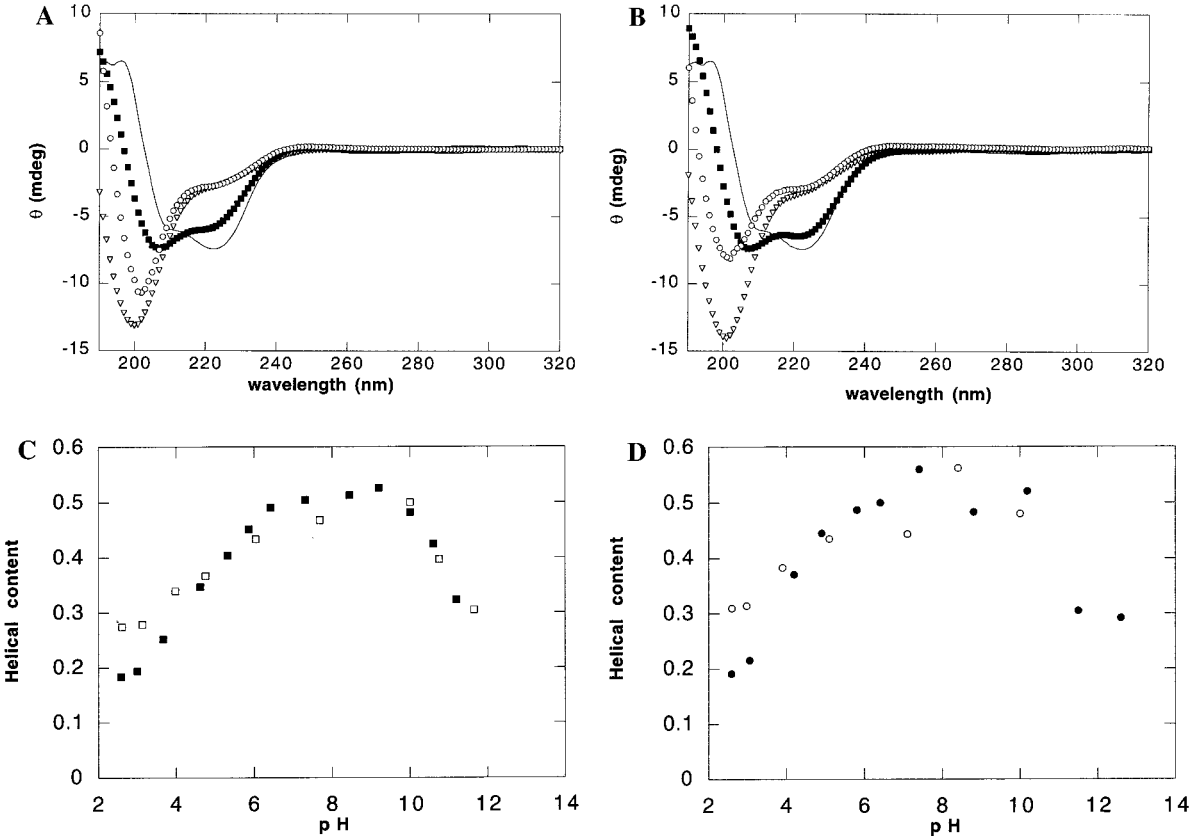

FIGURE 4: pH dependence of secondary structure in semisynthetic cytochrome *c* derivatives. Panels A and B show CD spectra of bpcc and phcc, respectively, at ~6 μM in ~10 mM sodium phosphate at pH values of 3 (▽), 7 (■), and 11 (○); the solid line shows the spectrum of holocytochrome *c* for comparison. Panels C and D show the calculated helix content of bpcc and phcc, respectively, as a function of pH. Closed symbols represent titration from low-pH to high-pH values, and open symbols represent back-titration. Helix content was calculated by the MLR method as described by Greenfield (*31*).

Structural Characterization of Biphenyl− and Phenanthrene−Cytochrome c Derivatives. pH titration of the two derivatives was monitored by CD. Figures 4A and 4B show the CD spectra at 20 °C for bpcc and phcc, respectively, at pH values of approximately 3, 7, and 11 in ~10 mM sodium phosphate buffer. At pH 7, both derivatives display negative minima near 208 and 222 nm and a positive maximum below 200 nm, indicating significant α-helical content. The spectra at pH 3 and pH 11 show a weaker shoulder shifted to around 228 nm and a minimum around 200 nm, indicating little or no secondary structure. The spectra at low pH values (<3) are similar to that for apocytochrome *c* (*15*), with little helical content [~18 ± 5%, calculated using all data from 190 to 240 nm using the method of nonconstrained least-squares analysis, referred to as the MLR method by Greenfield (*31*)]. The calculated helical content at each pH value is plotted in Figure 4C,D. The titrations for both derivatives are qualitatively and quantitatively similar, and show a largely reversible, bell-shaped pH dependence. A transition to higher helical content is observed with increasing pH values from ~2 to ~6, with a midpoint around pH 5 for either derivative. The transition reaches a plateau at pH ~6 to pH ~9 with maximum helical content of 50 ± 5%. Further titration to more basic pH reduces the helical content to ~30 ± 5% with a midpoint at pH ~9.5. At the most basic conditions, protein solutions are less transparent as judged by the base line of their UV−visible spectra, and precipitate over time; this may contribute to the incomplete reversibility of the pH titration. It also precludes the use of molar ellipticity in reporting the CD data in Figure 4A,B and in calculations of helix content in Figure 4C,D.

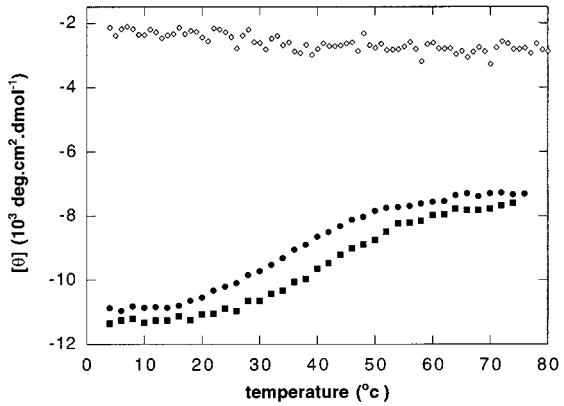

FIGURE 5: Temperature dependence of secondary structure in semisynthetic cytochrome *c* derivatives in 10 mM sodium phosphate, pH 6.0. The CD signal at 222 nm was monitored as a function of temperature with an automated gradient of approximately 1 °C per minute. Results are shown for 10.7 μM apocytochrome *c* (◇), 9.5 μM bpcc (●), and 6.4 μM phcc (■).

Figure 5 shows the thermal unfolding transitions of the two derivatives at pH 6, monitored by their CD signals at 222 nm. Both cytochrome *c* derivatives show nonlinear thermal transitions with well-developed pre- and post-transition base lines, in contrast to apocytochrome *c*, which shows only a barely sloping linear temperature dependence. The transition temperature of phcc (~45 °C) is slightly higher than that of bpcc (~35 °C). Each transition is reversible with

a similar transition temperature (not shown). However, the base lines after a heating and cooling cycle show lower CD signal intensities than those before the cycle, and reversibility defined by this measure declines as heating time increases. One reason for the difference in ellipticity between apocc and the derivatives at high temperature is the possibility of absorbance contributions from the surrogate groups at the single wavelength (222 nm) used to monitor the thermal transition; for this reason, the calculation of helix content from only this one wavelength would not provide a meaningful comparison among the three proteins, unlike the multiwavelength method used for calculation of helix content in the pH titration (see Materials and Methods). Additional contributing factors include the error in extinction coefficients of the derivatives, which limits the precision of concentration comparison, and the aggregation of the proteins at high temperatures, which is more severe for the two derivatives, leading to an increased base line signal relative to apocc.

Control experiments were carried out by CD difference titration (*37*) at pH 6 to determine if the surrogates influence the structure of apocytochrome *c* when not covalently attached. The spectrum of apocytochrome *c* was unaffected by addition of *m*,*m*′-dimethylbiphenyl at the highest accessible concentrations (~16 μM apocytochrome *c* and ~1.6 mM dimethylbiphenyl), indicating that, unlike heme (*15, 16*), the surrogates must be covalently attached to the cysteine side chains to influence protein secondary structure.

One-dimensional ^{1}H NMR spectra of the two derivatives at 0.2−0.3 mM, pH 6, 20 °C in D_2O show line broadening compared to spectra of apo- or holocytochrome *c* (not shown). The 1D spectra for both derivatives show normal line shapes for proteins of this size, indicating no significant oligomerization, which would have strongly broadened the lines. Amide exchange experiments for both bpcc and phcc monitored by 1D spectra showed no spectral changes, indicating that all amide protons were already exchanged within the dead time (~5 min). Two-dimensional HoMQC and NOESY spectra for either derivative do not show extensive cross-peaks among amide, α, and β protons. Although protein ^{1}H chemical shift assignments for either bpcc or phcc are not available, the lack of extensive cross-peaks suggests that the few observed correlations are intraresidue, and the line widths suggest the presence of states in intermediate conformational exchange on the NMR time scale.

DISCUSSION

In this work, two cytochrome *c* derivatives in which the covalently attached porphyrin group was substituted by surrogates differing in planarity were successfully produced through semisynthesis. Purification was accomplished by exploiting charge differences at pH 9, which are due to deprotonation of unreacted cysteine side chains. All analytical data on the products fit well to the expected attachment of one surrogate to two cysteine side chains of one protein molecule, consistent with the designed substitution of the porphyrin group. The structures and native-state stabilities of the two derivatives were compared with each other and with those for apocytochrome *c*, holocytochrome *c*, and porphyrin−cytochrome *c* in an effort to gain insight into the roles of covalent heme attachment.

The two derivatives, bpcc and phcc, both display significant pH-dependent secondary structure content without aggregation over the concentration range 6−300 μM. In contrast, pH titration of apocytochrome *c* in the absence of high salt shows no significant conformational changes between pH 2 and 8 and little helical content (*10*). Thus, despite their large differences from the porphyrin group, both surrogates used in the present work organize the protein chain into highly helical structures under conditions of physiological salt concentrations and pH values. Deconvolution of the CD spectra of bpcc and phcc indicates comparable maximum helical contents of ~50% and no protein concentration dependence in the range 6−35 μM. This helix content is similar to that of apocytochrome *c* in the presence of high concentrations of salt (*9*) and to that of porphyrin cytochrome *c* in physiological salt concentrations (*10*), conditions under which both proteins have been described as molten globules. This helix content is also comparable to that reported for native cyt *c*, although its spectra are somewhat different. Quantitative comparison of helix content in the various proteins is complicated by varying absorbance contributions of the attached groups in the far-UV region of the spectrum, which can lead to errors in calculating helix content, particularly from single-wavelength measurements. The method of calculating helix content used in the present work aims to minimize such errors by using all ellipticity data between 190 and 240 nm.

Both bpcc and phcc derivatives showed partly reversible pH titrations to forms with much lower helix content, with transitions at pH 5 and at pH 9.5. The acidic unfolding transition of the two derivatives resembles those of porphyrin−cyt *c* and holocytochrome *c* (*10*). The transition for porphyrin−cyt *c* shows similar steepness as the present derivatives, but with a midpoint at pH 3.5 (*10*). Similarly to the two heme surrogates, the porphyrin group does not retain the capability of iron ligation, but its two propionate groups may be involved in polar interactions with protein side chains. As expected, the transition for holocytochrome *c* shows the steepest transition and the lowest midpoint at pH 2.5. These results indicate that the two surrogates can stabilize helical structures in apocytochrome *c* similarly at neutral pH conditions, but the resulting structures are less stable to acid denaturation than those of porphyrin−cyt *c* or holocytochrome *c*. As the two surrogates lack any charged groups for interactions with protein side chains, their titration behavior implies that charged group interactions within the protein are important in stabilizing the helical structures formed at neutral pH.

A modified apocytochrome *c* produced by reacting 2 equiv of the hydrophobic fluorescent reagent I-AEDANS (5-[2-(2-iodoacetamido)ethylamino]-1-naphthalenesulfonic acid) with the cysteine side chains of apocytochrome *c* showed CD spectra that were similar to those of unmodified apocytochrome *c* at both pH 2 and pH 7 (*9*), suggesting that introduction of two AEDANS groups does not model the porphyrin very closely.

One-dimensional ^{1}H NMR spectra of the two derivatives at pH 6 show significant line broadening compared to that for apo- or holocytochrome *c*, indicative of intermediate conformational exchange. Similar line broadening was observed for porphyrin−cyt *c*, and was argued to indicate a resemblance to the molten globule states of holocytochrome

c obtained under low-pH conditions (*10*). The lack of cross-peaks in the NOESY spectra of bpcc and phcc is also similar to porphyrin−cyt *c*, and is consistent with high flexibility and/or short lifetime of individual conformations. All amide protons of the two derivatives studied here were exchanged within 5 min in hydrogen−deuterium exchange experiments, supporting the interpretation of a flexible and largely solvent-exposed structure.

Despite their flexibility, the two cytochrome *c* derivatives also show cooperative thermal transitions, with phcc slightly more stable than bpcc. The transitions are similar to those of ppcc at neutral pH (*10*), and show a prominent difference from that of apocc, which exhibits only a slight, linear change in CD signal. As expected, the steepness of the transition and the midpoint temperature for both derivatives and for ppcc are much lower than those of holocytochrome *c* under similar conditions (*38*), indicating that the folded structure in the derivatives and in ppcc is less stable and forms less cooperatively. Although the two derivatives showed little difference in pH titrations, in thermal melting phcc showed a slightly higher transition temperature than bpcc, suggesting that phenanthrene may better stabilize the folded state. The small difference may be due to the greater hydrophobicity or the more rigid aromatic ring of phenanthrene compared to biphenyl.

On the other hand, the comparable helical content of the two derivatives at low temperatures and at all pH values suggests that the functions of the two surrogates in organizing folded structure in the protein are similar. Thus, the additional conformational freedom of biphenyl compared with phenanthrene does not substantially reduce the stability of the structures formed in protein. It is striking that *both* heme surrogates studied here can induce helical structure in the protein to an extent comparable to that observed with covalently attached porphyrin itself, despite their much smaller size and the difference in rigid planarity between them. This finding suggests that the main similarity between the porphyrin group and the two surrogates—their hydrophobicity—is the dominant factor in the ability of these covalently attached groups to organize helical structure in the protein.

ACKNOWLEDGMENT

We thank Prof. Robert A. Pascal, Jr., for his insight and assistance in the design and synthesis of the two surrogates. We also thank István Pelczer, Monty Scott, and Aparna Kesarwala for their contributions to this work, and Ingrid Hughes for assistance with the manuscript.

SUPPORTING INFORMATION AVAILABLE

HoMQC spectra and a table of chemical shift assignments are available as supporting information (3 pages). This material is available free of charge via the Internet at http://pubs.acs.org.

REFERENCES

1. Dickerson, R. E., Takano, T., Eisenberg, D., Kallai, O. B., Samson, L., Cooper, A., and Margoliash, E. (1971) Ferricytochrome *c*, general features of the horse and bonito proteins at 2.8 A resolution. *J. Biol. Chem. 246*, 1511−1535.
2. Bushnell, G. W., Louie, G. V., and Brayer, G. D. (1990) High-resolution three-dimensional structure of horse heart cytochrome *c*. *J. Mol. Biol. 214*, 585−595.
3. Qi, P. X., Beckman, R. A., and Wand, A. J. (1996) Solution structure of horse heart ferricytochrome *c* and detection of redox-related structural changes by high-resolution 1H NMR. *Biochemistry 35*, 12275−12286.
4. Banci, L., Bertini, I., Gray, H. B., Luchinat, C., Reddig, T., Rosato, A., and Turano, P. (1997) Solution structure of oxidized horse heart cytochrome *c*. *Biochemistry 36*, 9867−9877.
5. Gonzales, D. H., and Neupert, W. (1990) Biogenesis of mitochondrial *c*-type cytochromes. *J. Bioenerg. Biomembr. 22*, 753−768.
6. Stellwagen, E., Rysavy, R., and Babul, J. (1972) The conformation of horse heart apocytochrome *c*. *J. Biol. Chem. 247*, 8074−8077.
7. Fisher, W. R., Taniuchi, H., and Anfinsen, C. B. (1973) On the role of heme in the formation of the structure of cytochrome *c*. *J. Biol. Chem. 248*, 3188−3195.
8. Kutyshenko, V. P. (1990) High resolution ^{1}H NMR study of equine heart apocytochrome *c*. *Biofizika 35*, 407−409.
9. Hamada, D., Hoshino, M., Kataoka, M., Fink, A. L., and Goto, Y. (1993) Intermediate conformational states of apocytochrome *c*. *Biochemistry 32*, 10351−10358.
10. Hamada, D., Kuroda, Y., Kataoka, M., Aimoto, S., Yoshimura, T., and Goto, Y. (1996) Role of heme axial ligands in the conformational stability of the native and molten globule states of horse cytochrome *c*. *J. Mol. Biol. 256*, 172−186.
11. Falzone, C. J., Mayer, M. R., Whiteman, E. L., Moore, C. D., and Lecomte, J. T. J. (1996) Design challenges for hemoproteins: the solution structure of apocytochrome b_5. *Biochemistry 35*, 6519−6526.
12. Feng, Y., Sligar, S. G., and Wand, A. J. (1994) Solution structure of apocytochrome b_{562}. *Struct. Biol. 1*, 30−35.
13. Eliezer, D., and Wright, P. E. (1996) Is apomyoglobin a molten globule? Structural characterization by NMR. *J. Mol. Biol. 263*, 531−538.
14. Eliezer, D., Yao, J., Dyson, H. J., and Wright, P. E. (1998) Structural and dynamic characterization of partially folded states of apomyoglobin and implications for protein folding. *Nat. Struct. Biol. 5*, 148−155.
15. Dumont, M. E., Corin, A. F., and Campbell, G. A. (1994) Noncovalent binding of heme induces a compact apocytochrome *c* structure. *Biochemistry 33*, 7368−7378.
16. Goldberg, M. E., Schaeffer, F., Guillou, Y., and Djavadi-Ohaniance, L. (1999) Pseudo-native motifs in the noncovalent heme−apocytochrome *c* complex: Evidence from antibody binding studies by ELISA and microcalorimetry. *J. Biol. Chem. 274*, 16052−16061.
17. LaMar, G. N., Davis, N. L., Parish, D. W., and Smith, K. M. (1983) Heme orientational disorder in reconstituted and native sperm whale myoglobin. *J. Mol. Biol. 168*, 887−896.
18. McLachlan, S. J., LaMar, G. N., Burns, P. D., Smith, K. M., and Langry, K. C. (1986) ^{1}H NMR assignments and the dynamics of interconversion of the isomeric forms of cytochrome b5 in solution. *Biochim. Biophys. Acta 874*, 274−284.
19. Moore, G. R., and Pettigrew, G. W. (1990) in Cytochromes *c*: Evolutionary, structural and physicochemical aspects, pp 116−125, Springer-Verlag, Berlin.
20. Tanaka, Y. Ashikari, T., Shibano, Y., Amachi, T., Yoshizumi, H., and Matsubara, H. (1988) Amino acid replacement studies of human cytochrome *c* by a complementation system using CYC1 deficient yeast *J. Biochem. 104*, 477−480.
21. Tanaka, Y. Kubota, I., Amachi, T., Yoshizumi, H., and Matsubara, H. (1990) Site-directly mutated human cytochrome *c* which retains heme *c* via only one thioether bond. *J. Biochem. 108*, 7−8.
22. Hobbs, J. D., and Shelnutt, J. A. (1995) Conserved nonplanar heme distortions in cytochromes *c*. *J. Protein Chem. 14*, 19−25.
23. Pace, C. N., Grimsley, G. R., Thomson, J. A., and Barnett, B. J. (1988) Conformational stability and activity of ribonuclease

T1 with zero, one, and two intact disulfide bonds. *J. Biol. Chem. 263*, 11820−11825.
24. Fitch, W. (1976) The molecular evolution of cytochrome *c* in eukaryotes. *J. Mol. Evol. 8*, 13−40.
25. Brems, D. N., and Stellwagen, E. (1983) Conformational transitions of a cytochrome *c* having a single thioether bridge. *J. Biol. Chem. 258*, 10919−10923.
26. Scott, J. M. (1995) Substitution of bromomethyl analogues for the protoporphyrin IX heme group in cytochrome *c*. Bachelor Thesis, Princeton University.
27. Hu, S., Morris, I. K., Singh, J. P., Smith, K. M., and Spiro, T. G. (1993) Complete assignment of cytochrome *c*. Resonance Raman spectra via enzymatic reconstitution with isotopically labeled hemes. *J. Am. Chem. Soc. 115*, 12446−12460.
28. Zahler, W. L., and Cleland, W. W. (1968) A specific and sensitive assay for disulfides. *J. Biol. Chem. 243*, 716−719.
29. Rosen, H. (1957) A modified ninhydrin colorimetric analysis for amino acids. *Arch. Biochem. Biophys. 67*, 10−15.
30. Kang, X. (1999) Protein folding studied by semisynthesis: the role of heme in structural organization of horse heart cytochrome *c*. Ph.D. Thesis, Princeton University.
31. Greenfield, N. J. (1996) Methods to estimate the conformation of proteins and polypeptides from circular dichroism data. *Anal. Biochem. 235*, 1−10.
32. Pelczer, I., and Bishop, K. D. (1997) Optimal acquisition and presentation of HoMQC spectra in *Methods for structure elucidation by high-resolution NMR* (Batta, G., Köver, K. E., and Szántay, C., Jr., Eds.) pp 187−207, Elsevier, New York.
33. Jeener, J., Meier, B. H., Bachman, P., and Ernst, R. R. (1979) Investigation of exchange processes by two-dimensional NMR spectroscopy. *J. Chem. Phys. 71*, 4546−4553.
34. Piotto, M., Saudek, C., and Sklenar, V. (1992) Gradient-tailored excitation for single-quantum NMR spectroscopy of aqueous solutions. *J. Biomol. NMR 2*, 661−665.
35. Delaglio, F., Grzesiek, S., Vuister, G. W., Zhu, G., Pfeifer, J., and Bax, A. (1995) NMRPipe: A multidimensional spectral processing system based on UNIX pipes. *J. Biomol. NMR 6*, 277−293.
36. Johnson, B. A., and Belvins, R. A. (1994) NMRView: A computer program for the visualization and analysis of NMR data. *J. Biomol. NMR 4*, 603−614.
37. Kang, X., and Carey, J. (1999) Structural organization in peptide fragments of cytochrome *c* by heme binding. *J. Mol. Biol. 285*, 463−468.
38. Hagihara, Y., Tan, Y., and Goto, Y. (1994) Comparison of the conformational stability of the molten globule and native states of horse cytochrome *c*. *J. Mol. Biol. 237*, 336−348.
39. Koradi, R., Billeter, M., and Wüthrich, K. (1996) MOLMOL: A program for display and analysis of macromolecular structures. *J. Mol. Graph. 14*, 51−55.

BI9919089